Research Square

Preprints are preliminary reports that have not undergone peer review.
They should not be considered conclusive, used to inform clinical practice,
or referenced by the media as validated information.

Serine determines tissue targeted efficacy of PKM2 modulators in atopic dermatitis

Luke O'Neill

laoneill@tcd.ie

Trinity College Dublin https://orcid.org/0000-0002-4333-2748

Tom Ashton

Sitryx Therapeutics

Sabine Broc

Sitryx Therapeutics

Gareth Davies

Sitryx Therapeutics https://orcid.org/0000-0001-5180-3143

Martin Domville

Sitryx Therapeutics

Marina Makrecka

Sitryx Therapeutics

Hamel Patel

Sitryx Therapeutics

Angharad Fenton-May

Sitryx Therapeutics

Neil Bennett

Sitryx Therapeutics

Kimberly Herman

Sitryx Therapeutics

Marie Strickland

Sitryx Therapeutics

Eva Palsson-McDermott

Trinity College Dublin

Daniel Jupp

Sitryx Therapeutics

Oscar Barba

Sitryx Therapeutics

Alessandro Mazzacani

Sitryx Therapeutics

Mark Whitmarsh

Sitryx Therapeutics
Lisa Pierre
Sitryx Therapeutics
Ravi Rao
Sitryx Therapeutics
Iain Kilty
Sitryx Therapeutics

Article

Keywords:

Posted Date: July 25th, 2026

DOI: https://doi.org/10.21203/rs.3.rs-9496359/v1

License: This work is licensed under a Creative Commons Attribution 4.0 International License.
Read Full License

Additional Declarations: Yes there is potential Competing Interest. Luke O'Neill is a founder of of Sitryx Therapeutics. All other authors are employees of Sitryx Therapeutics. Sitryx Therapeutics is developing PKM2 modulators for the treatment of inflammatory diseases. All authors may hold stock options in Sitryx Therapeutics.

Abstract

Pyruvate kinase M2 (PKM2) is a key glycolytic enzyme that regulates immune cell activation, and PKM2 activators such as the literature tool compound, TEPP-46, have shown that targeting PKM2 is immunomodulatory. However, previous studies reveal a disconnect between TEPP-46 potency in cellular assays and efficacy in animal models of inflammation or autoimmunity. This study identifies serine demand as a factor responsible for this disconnect and the key determinant of the cellular and tissue-level response to PKM2 modulation.

SYX-PKM-A is a novel orally bioavailable PKM2 modulator that induced tetramer formation and increased pyruvate kinase activity in human lymphocytes. PKM2 activation redirects 3-phosphoglycerate (3-PG) away from serine biosynthesis, limiting one-carbon metabolism and nucleotide production. This induces a state of serine auxotrophy in activated human $CD4^+$ T cells, Th2 cells, Th17 cells, and B cells, leading to reduced proliferation, cytokine release and immunoglobulin production. These effects are dependent on serine concentration and fully rescued by exogenous formate, confirming one-carbon pathway restriction as the primary mechanism.

Skin from atopic dermatitis (AD) patients exhibits reduced serine, increased PKM2, and upregulation of serine transporters and one-carbon metabolism genes, indicating a high serine-demand environment with PKM2-driven metabolic vulnerability. Consistent with this, SYX-PKM-A demonstrates robust efficacy in DNFB-induced dermatitis, KLH delayed-type hypersensitivity, and chronic house dust mite models, reducing lymphocytes, Th2 cytokines, and tissue inflammation to levels comparable with JAK inhibition.

These findings establish serine-dependent metabolic restriction as a mechanism for tissue-targeted immunoregulation and highlight PKM2 modulation as a promising oral therapeutic strategy for AD and other T cell–driven inflammatory diseases.

Introduction

Pyruvate kinase (PK), as one of the key enzymes of glycolysis, acts on its substrate phosphoenolpyruvate (PEP) to form pyruvate [1]. Monomeric and dimeric PKM2 have low affinity to PEP and exhibit minimal catalytic activity, whereas tetrameric PKM2 has high affinity to PEP and high catalytic activity [2,3]. Although the canonical function of PKM2 is in glycolysis, non-canonical functions of the dimer have also been described in disease states, including nuclear translocation and upregulation of pro-inflammatory gene transcription. PKM2 is upregulated in a range of cancers, inflammatory and auto-immune diseases and is therefore a target of therapeutic interest [1,4]. Dimeric PKM2 is upregulated in stimulated murine and human CD4 T cells, promoting proliferation and inflammatory cytokine release. The literature tool PKM2 activator, TEPP-46, induces formation of anti-inflammatory PKM2 tetramers in stimulated CD4 T cells, Th1 and Th17 cells at high concentrations of 50 μM and above, blocking proliferation and cytokine release [5–8]. However, the impact of PKM2 modulators has not been explored in T cells treated *in vitro* at concentrations that can be achieved *in vivo.* Furthermore, no studies have

tested PKM2 modulation in B cells, despite the known elevation of PKM2 expression and activity in B cell-related diseases such as hyperhomocysteinemia-accelerated atherosclerosis, Burkitt's lymphoma and diffuse large B cell lymphoma [9–11].

In cancer cell lines, PKM2 activators, including TEPP-46, channel the glycolytic intermediate 3-PG towards pyruvate production, reducing carbon flux through the serine biosynthesis pathway [12,13]. There is a similar finding in Ova-activated T cell receptor transgenic mouse CD8 + T cells, albeit following treatment with 60 μM TEPP-46, which can't be achieved *in vivo* [14]. A downstream effect of this reduced flux is a decrease in purine synthesis resulting in impaired cell proliferation. Inhibition of serine biosynthesis can also decrease protein synthesis because serine is an amino acid precursor of glycine, cysteine and methionine [15]. These effects would explain why the pharmacological activity of TEPP-46 is revealed under low serine conditions in cancer cell lines [12,13]. However, the impact of PKM2 modulators on human lymphocytes have not been explored in environments with high serine demand.

T and B cells require serine to fuel one carbon metabolism and downstream protein synthesis and nucleotide biosynthesis. These are essential processes to maintain proliferation and adequate immune responses [16–20]. Serine is a non-essential amino acid that may either be synthesised *de novo* or imported from the extracellular environment. 20% of the serine pool in activated human effector T cells is derived from *de novo* serine biosynthesis, whereas 80% of serine is taken from the extracellular environment, highlighting the importance of serine import [16]. A hallmark of increased serine demand in lymphocytes is elevated expression of *de novo* serine biosynthesis enzymes, including PHGDH, PSAT1 and PHGDH [17,20]. These enzymes are increased in activated B cells, tonsils of cancer-free individuals and in mouse GC B cells following challenge with sheep red blood cells. In addition, these serine biosynthesis enzymes are upregulated in germinal centre B cell-derived lymphomas and correlate with poorer overall survival. Conditional knockout or inhibition of PHGDH in lymphoma cells impairs proliferation, induces apoptosis and limits disease progression in a mouse lymphoma transplantation model, identifying this pathway as a therapeutic target [17]. Therefore, activated lymphocytes have a high level of both *de novo* serine synthesis and serine import to support serine demand for proliferation and inflammatory processes.

There is an emerging critical role of serine in maintaining normal tissue function. Serine deficient mice have delayed hair regeneration and accelerated re-epithelialization, causing improper wound healing [21]. In addition, high serine demand has been described in other inflammatory diseases such as psoriasis, Crohn's disease, ulcerative colitis and rheumatoid arthritis [22,23]. In psoriasis, high levels of serine synthesis correlate with a decrease in skin serine levels compared to healthy controls. Correspondingly, serine synthesis enzymes have increased expression in colon epithelia of Crohn's disease, ulcerative colitis and murine models of colitis [24]. Serine is also significantly reduced in a collagen-induced arthritis mouse model plasma compared to controls, and low plasma serine correlates with high disease activity in rheumatoid arthritis [25,26]. Therefore, high serine demand could be a metabolic vulnerability open to therapeutic intervention in inflammatory indications.

Atopic dermatitis (AD) is a complex, chronic inflammatory, non-contagious skin disease with high unmet need and no curative treatment options. It is the most common inflammatory skin disorder in the developed world with a lifetime prevalence of 15–20% [27,28]. Disease pathogenesis arises from genetic, immunological, and environmental factors, which result in defects to the epidermal barrier and immune dysregulation. Th2 cells are the key driver of AD, releasing IL-4 and IL-13 to promote IgE class switching in B cells [29]. There is also involvement of Th1 and Th17 cells in chronic disease. The approved JAK inhibitors, upadacitinib, abrocitinib and baricitinib have good efficacy in AD but are generally reserved for use in moderate-to-severe AD patients for whom other systemic therapies have failed to be effective. s. Despite the recent approvals of biologics targeting the IL-4/IL-13pathway, dupilumab, tralokinumab and lebrikizumab, there remainssignificant unmet need and no safe and well tolerated approved oral treatment option. Therefore, PKM2 modulation would be a novel therapeutic strategy predicted to be efficacious in T cell driven diseases such as AD.

This study describes a novel PKM2 modulator, SYX-PKM-A, which induced serine auxotrophy in human lymphocytes by channeling the glycolytic intermediate, 3-phosphoglycerate (3-PG) towards pyruvate production, reducing carbon flux through serine biosynthesis. This, combined with low-serine culture conditions, resulted in anti-inflammatory activity on human Th2, Th17 and IgE-expressing B cells, which play a crucial role in the pathogenesis of AD. These findings identify serine demand as the factor responsible for the disconnect between PKM2 modulator potency in cellular assays and efficacy in animal models of inflammation or autoimmunity. SYX-PKM-A was efficacious in multiple T cell driven animal models, demonstrating impact on readouts including inflammation, lymphocytes and Th2 cytokines. Characterisation of AD skin revealed elevated PKM2 expression and high serine demand, presenting a metabolic vulnerability for therapeutic intervention with a novel PKM2 modulator. The tissue-targeted efficacy of PKM2 modulation at AD inflammatory sites enables a differentiated safety profile and could address the major unmet needs of AD as a safe, convenient and effective therapy where there are limited treatment options under the current standard of care.

Results

A novel small molecule activates PKM2 in human CD4+ T cells

The small molecule TEPP-46 has been widely used to investigate PKM2 modulation in cancer cell lines and inflammatory T cells [5–7]. PKM2 modulators such as TEPP-46 promote the conversion of dimeric, catalytically inactive PKM2 to tetrameric, catalytically active PKM2 [2,3,30]. The TEPP-46 binding site is predominantly hydrophobic, favouring flat aromatic scaffolds that reinforce subunit assembly by π–π stacking with the protein and van der Waals interactions (PDB ID: 3u2z; Supplementary Figure 1A) [31]. The requirement for high aromaticity and lipophilicity typically results in ligands exhibiting poor aqueous solubility and suboptimal physicochemical properties that adversely affect pharmacokinetic parameters, such as oral exposure and bioavailability.

We sought to develop novel small molecule PKM2 activators suitable for oral treatment of inflammatory diseases. A new series of phthalazinone derivative PKM2 activators able to promote tetramerization [32], was conceived through a structure-guided design strategy, using information on the topology and physicochemical features of the allosteric pocket located at the twofold symmetric interface of the PKM2 tetramer [33].

To initiate the medicinal chemistry campaign, we developed structure-based docking models derived from the crystallographic data both generated in house and available in the literature. These models provided a structural framework for ligand design and optimisation, allowing exploration of substituents capable of engaging the hydrophobic residues that define the allosteric pocket. Guided by these insights, the design strategy focused on scaffolds predicted to retain the key π–π stacking and van der Waals interactions required for effecting binding mode. Hence, the novel phthalazinone core perfectly occupies a shallow hydrophobic cavity bordered by residues Phe26, Leu27, and Tyr390 with the minimal number of aromatic rings. Substituent patterns were designed to preserve key interactions within the lipophilic cleft while maintaining acceptable overall lipophilicity and permeability.

Improving physicochemical properties and solubility to support oral bioavailability was key in the lead optimisation phase. Iterative modelling and property-based optimisation were employed to achieve an effective balance between enzyme activation and physicochemical tractability.

This approach led to the discovery of SYX-PKM-A (Figure 1A; Figure 1B) as an orally available PKM2 modulator candidate with suitable physiochemical, ADME and pharmacokinetic properties (Table 1, Supplementary Figure 1B).

		SYX-PKM-A
MW		341.41
Molecular formula		$C_{18}H_{15}N_5O_3S$
Thermodynamic Solubility in Fed State Simulated Intestinal Fluid (FaSSIF) media (μM)		125
Measured LogD (shake flask)		1.7
Topological Polar Surface Area ($Å^2$)		116.8
Mouse plasma protein binding (Fu)		0.13
Human plasma protein binding (Fu)		0.10
Caco2 Permeability	Papp A→B ($\times 10^{-6}$ cm/s)	8.89
	Papp B→A ($\times 10^{-6}$ cm/s)	39.75
	Efflux Ratio (B→A / A→B)	4.47
Mouse plasma pharmacokinetic parameters (1 mg/kg IV)	CL (mL/min/kg)	10.2
	Vss (L/kg)	1.78
	$T_{1/2}$ (hours)	4.2
	Unbound C_{max} (μM)	0.38
	Unbound AUC_{INF} (hours*ng/mL)	220
Mouse plasma pharmacokinetic parameters (60 mg/kg PO)	T_{max} (hours)	0.5
	Unbound C_{max} (μM)	11.6
	$T_{1/2}$ (hours)	2.5
	Unbound AUC_{INF} (hours*ng/mL)	11162

Table 1 – Physicochemical, ADME, and mouse pharmacokinetic properties of SYX-PKM-A.

SYX-PKM-A increased PKM2 catalytic activity with EC_{50} values of 138 nM for human recombinant PKM2 and 304 nM for mouse recombinant PKM2, reaching an Emax comparable with 5 μM TEPP-46 (Figure 1C and 1D). An increase in pyruvate kinase activity was also observed following treatment of human CD4+ T cells with SYX-PKM-A with an EC_{50} of 66 nM, reaching an Emax comparable with 30 μM TEPP-46 (Figure 1E). The potency of TEPP-46 in these assays was similar to SYX-PKM-A.

As discussed, PKM2 exists in equilibrium between monomeric, dimeric, and tetrameric forms. To study the impact of PKM2 activators on this equilibrium in cells, LPS stimulated bone marrow derived

macrophages were treated with 30 μM TEPP-46 or 1 μM SYX-PKM-A. Cell lysates were then treated with disuccinimidyl suberate, used as an amine-reactive crosslinker that links lysine side chains to capture all PKM2 oligomeric species [5,34]. PKM2 western blotting revealed that TEPP-46 and SYX-PKM-A increased PKM2 tetramer (Figure 1F).

Collectively these results indicated that SYX-PKM-A is a cell-permeable PKM2 activator with drug-like properties, able to effectively promote PKM2 tetramerisation, ultimately resulting in increased pyruvate kinase activity in CD4+ T cells.

PKM2 modulation induces serine auxotrophy in human CD4+ T cells

TEPP-46 is widely used as a PKM2 modulator for *in vitro* studies in the fields of cancer and inflammation, typically tested at 50 to 100 μM [1,5–7,30,34–36]. In our study the unbound C_{max} of TEPP-46 following PO delivery of a single 3 mg/kg dose in C57BL/6 mice was 489 nM (Supplementary Figure 1B). The previously reported C_{max} of TEPP-46 following PO delivery of a single 10 mg/kg dose in BALB/c mice was 3.5 μM once corrected for fraction unbound (Fu) of 0.1286% determined by mouse plasma protein binding [30]. Therefore, many of the published *in vitro* studies are difficult to interpret because TEPP-46 is used at concentrations that can't be achieved *in vivo*. Furthermore, the potency of TEPP-46 in the human CD4+ T cell pyruvate kinase assay is 86 nM (Figure 1E), revealing a disconnect between the low nanomolar concentrations required for target engagement and the micromolar concentrations typically used to elicit immunomodulatory effects *in vitro* under standard culture conditions. We examined serine as a potential factor responsible for this disconnect in inflammation.

Traditional culture media were developed to support a high level of cell growth rather than to model the metabolic composition of human tissue and standard Roswell Park Memorial Institute (RPMI) contains 280 μM serine, which is supra-physiological [37]. TEPP-46 induces serine auxotrophy in cancer cell lines by channelling the glycolytic intermediate, 3-PG towards pyruvate production, reducing carbon flux through serine biosynthesis and impairing cell proliferation in media containing between 0 and 30 μM serine [12,13]. A similar anti-proliferative effect was observed in A549 human lung adenocarcinoma cells incubated with TEPP-46 or SYX-PKM-A in 20 μM serine media without causing toxicity (Supplementary Figures 1C and 1D). This finding has only been previously explored in cancer cell lines. To investigate the impact of PKM2 modulation in inflammatory immune cells, human CD4+ T cells were stimulated with αCD3/αCD28 beads for 5 days in 10 μM low serine media. In accordance with previously published findings [5–7], PKM2 expression was increased by stimulation (Supplementary Figure 2A). In low serine media, an anti-proliferative effect was observed with an IC_{50} of 5 nM for SYX-PKM-A and 4 nM for TEPP-46, whereas no significant decrease in proliferation was observed in 100 μM high serine media (Figure 2A, Figure 2B). Cell viability was unaffected by treatment (Supplementary Figure 2B).

Serine is a known allosteric activator of recombinant PKM2 with a half maximal activation concentration of 1.3 mM [38,39]. In cells however, allosteric regulation of PKM2 by glycolysis-derived fructose 1,6-bisphosphate (FBP) is dominant over serine, even with addition of 5 mM exogenous serine [40]. In agreement with these findings, 10 mM serine alone only partially activated human recombinant PKM2 with an Emax of 28% compared to SYX-PKM-A alone (Figure 2C). Addition of serine did not alter the EC_{50} or Emax of SYX-PKM-A. This revealed a lack of functional allosteric interaction between SYX-PKM-A and serine.

Consequently, the observed anti-proliferative effect is more likely to be caused by reduced flux through serine biosynthesis than allosteric effects of serine on PKM2. This was investigated by stimulation of CD4+ T cells with αCD3/αCD28 beads for 2 days followed by addition of heavy labelled α-15N L-glutamine for 24 hours in glutamine-free media. Label incorporation into the *de novo* serine biosynthesis metabolite, phosphoserine +1, and downstream purine synthesis derived ATP +2 was significantly decreased by SYX-PKM-A (Figure 2D). SYX-PKM-A did not cause a decrease in high serine media (Supplementary Figure 2C). This suggested that SYX-PKM-A decreases *de novo* serine biosynthesis flux and purine synthesis. In support of this finding, pyrimidines such as deoxyuridine, thymidine and deoxycytidine, likely derived from the extracellular environment, were increased by SYX-PKM-A, whereas intracellular synthesis of ribonucleotides and deoxyribonucleotides were decreased (Figure 2E).

Maintenance of intracellular serine homeostasis is a balance between *de novo* serine biosynthesis and serine import from the extracellular environment. Inflammatory T cells and B cells are highly dependent on serine for proliferation and function, and therefore in a high serine demand environment, elevated expression of plasma membrane serine transporters, *de novo* serine biosynthesis enzymes and one carbon metabolism enzymes is expected [16–20]. Accordingly, in human Th2 cells cultured in low serine, serine transporters (SLC1A4, SLC1A5) and the *de novo* serine synthesis enzyme, PHGDH, were upregulated by stimulation (Figure 2F). SLC1A4, PHGDH and one carbon metabolism enzyme, SHMT1 were further upregulated by SYX-PKM-A, consistent with restricted flux through *de novo* serine synthesis resulting in compensatory elevation in expression of pathway enzymes and serine transporters (Figure 2G).

The mTOR inhibitor, rapamycin, inhibits CD4+ T cell proliferation [41] and had an anti-proliferative effect comparable with SYX-PKM-A (Figure 2A). This effect is largely due to inhibition of S6K1 and 4E-BP1 phosphorylation, reduced Myc expression and decreased expression of glucose transporters, and is independent of one carbon metabolism. Interestingly rapamycin caused a decrease in expression of *de novo* serine synthesis, serine transporter and one carbon metabolism genes (Figure 2G). This indicated that the mechanism responsible for the anti-proliferative effect of rapamycin is independent of suppression in serine biosynthesis flux.

Formate is a one carbon metabolism intermediate and precursor for the *de novo* synthesis of purine nucleotides [19]. The anti-proliferative effect of SYX-PKM-A correlated with a decrease in formate release, providing further evidence that SYX-PKM-A causes a decrease in one carbon metabolism activity (Figure

2H). Addition of exogenous formate to CD4+ T cells stimulated in low serine media resulted in near complete rescue of the anti-proliferative effect of SYX-PKM-A. This revealed that the principal driver of this phenotype is inhibition of one carbon metabolism (Figure 2I).

Collectively these results indicated that in a high serine demand environment, PKM2 modulation by SYX-PKM-A channels 3-PG towards pyruvate production in human CD4+ T cells, restricting flux of metabolic intermediates through serine biosynthesis. There is a corresponding limitation in downstream flux through one carbon metabolism, resulting a diminished nucleotide pool and decreased cell proliferation (Figure 2J). There is a compensatory increase in expression of one carbon metabolism enzymes, serine biosynthesis enzymes and plasma membrane serine transporters in an attempt to maintain high intracellular serine.

PKM2 modulation inhibits human Th2 and Th17 cell function

Th2 cells are the key driver of AD, releasing pro-inflammatory cytokines including IL-13 and IL-31 [29]. PKM2 modulation has not been studied in Th2 polarising conditions. Therefore, naïve CD4+ T cells were stimulated for 5 days with αCD3/αCD28 beads, αIFNγ, IL-2 and IL-4 in low serine conditions, resulting in upregulation of PKM2 (Supplementary Figure 2D). Expression of the Th2 transcription factor, GATA3 [42], was increased from 16 ± 1% to 82 ± 8% (mean ± SEM), demonstrating efficient polarisation (Supplementary Figure 2E). When cells were treated with SYX-PKM-A for the duration of the culture, an anti-proliferative effect was observed in low serine conditions with an IC_{50} of 5 nM, similar to the potency in total CD4+ T cells (Figure 3A). SYX-PKM-A also inhibited release of IL-13 and IL-31 with a maximal decrease of 63% compared to a 43% decrease in proliferation (Figure 3B). This was not observed in high serine media and viability was unaffected (Figure 3C; Supplementary Figure 2F). The rapamycin positive control caused a similar decrease in IL-13 and IL-31 release. The anti-proliferative effect of SYX-PKM-A correlated with a decrease in formate release, providing further evidence that SYX-PKM-A causes a decrease in one carbon metabolism activity (Supplementary Figure 2G).

Th17 and Th1 cells contribute to chronic AD, releasing pro-inflammatory cytokines including IL-17A and IFNγ, respectively [29]. High concentration TEPP-46 decreases proliferation and IL-17A expression in mouse Th17 cells in supra-physiological serine conditions [35]. To examine the impact of PKM2 modulation on human Th17 cells in low serine conditions, memory CD4+ T cells were stimulated for 6 days with αCD28, αIFNγ, αIL-4, IL-1β, IL-2 and IL-23. There was a significant increase in IL-17A release compared to αCD28 stimulation alone, indicating efficient polarisation (Figure 3E). SYX-PKM-A treatment throughout the culture led to a decrease in proliferation with an IC_{50} of 1 nM and a comparable decrease in IL-17A release with an IC_{50} of 2 nM (Figure 3D and 3E). The rapamycin positive control also caused decreases in proliferation and release of IL-17A.

Td-IPV (REVAXIS) is an inactivated vaccine containing diphtheria toxoid, tetanus toxoid and inactivated poliovirus, widely used in Europe as a booster in adolescents and adults. Vaccine antigens can be used *in vitro* to induce a more physiological antigen-specific memory CD4+ T cell recall response in adult PBMC donors [43]. PBMCs were stimulated with Td-IPV and IL-2 for 13 days in low serine media. The calcineurin inhibitor, cyclosporin A, was used as a positive control and caused significant decreases in proliferation and IFNγ release (Figure 3F and 3G). SYX-PKM-A treatment throughout the culture led to a dose dependent decrease in proliferation and a comparable decrease in IFNγ release.

These data demonstrated the potential of SYX-PKM-A to dampen the proliferation and function of Th2, Th17 and IFNγ-releasing cells in AD for therapeutic benefit.

PKM2 modulation inhibits human B cell function

B cell PKM2 expression and activity is elevated in hyperhomocysteinemia-accelerated atherosclerosis, Burkitt's lymphoma and diffuse large B cell lymphoma [9–11]. However, PKM2 activators have not been studied in B cells. To investigate the impact of PKM2 modulation on human B cells in low serine conditions, peripheral B cells were differentiated for 7 days with MegaCD40L, anti-B cell receptor, IL-2 and IL-21 to promote IgG release and treated with SYX-PKM-A throughout. A METAP2 inhibitor was used as an assay positive control [44], resulting in decreases in proliferation and IgG release (Figure 4B). PKM2 modulation caused a decrease in the CD20- CD27+ CD38+ CD138- plasmablast population with an IC_{50} of 0.4 nM (Figure 4A and 4B). Furthermore, IgG release was inhibited with an IC_{50} of 2 nM (Figure 4C). This effect was not observed in high serine media and was almost completely rescued by exogenous formate, demonstrating that one carbon metabolism is also inhibited in B cells by SYX-PKM-A. Despite the decrease in the number of plasmablasts, the plasmablast division index was unaffected, suggesting that fewer B cells differentiate into plasmablasts, but the division of these plasmablasts is normal (Figure 4D). There was no impact of PKM2 modulation on CD38- CD20+ CD27+ memory B cells (Figure 4E).

Serum IgE is elevated in AD patients who have a strong systemic allergic component and dendritic cells harbouring IgE receptors are increased in AD skin [27,29]. To examine the specificity of PKM2 modulation for IgG, B cells were differentiated for 7 days in low serine media with MegaCD40L, IL-2, IL-4, IL-13 and IL-21 to promote IgE release. Similar to the effect on IgG, SYX-PKM-A inhibited IgE release with an IC_{50} of 1 nM in low serine media but not in high serine media (Figure 4F). In contrast with the IgG assay, plasmablast numbers were unaffected (Figure 4G).

Taken together with the T cell findings, these data indicate that PKM2 modulation inhibits flux through serine biosynthesis and downstream one carbon metabolism in lymphocytes. In T cells the key impact is on nucleotide synthesis to support proliferation and in B cells the key impact is on serine as an amino acid precursor of glycine, cysteine and methionine to support antibody synthesis.

PKM2 modulation is efficacious in a mouse model of skin inflammation in which serine is limiting

The mouse 2,4 dinitrofluorobenzene (DNFB) skin inflammation model was selected to investigate SYX-PKM-A *in vivo* pharmacology because it shows substantial transcriptional concordance with human atopic dermatitis, with 33% of differentially expressed genes in this model shared with the human meta-analysis derived atopic dermatitis transcriptome, which was superior to all other models tested [45]. BALB/c mice were sensitised with DNFB on the back skin on days 0 and 1, followed by DNFB challenge on the ear on day 5. Serine measured in the ear tissue was decreased 24 hours after DNFB challenge compared to ear tissue from naïve animals, establishing this as a suitable inflammatory skin model with high serine demand in tissue (Figure 5A). SYX-PKM-A and baricitinib were administered orally BID throughout the model at the doses indicated. SYX-PKM-A treatment resulted in a dose-dependent decrease in ear thickness indicating a reduction in inflammation, which at the 3 mg/kg SYX-PKM-A BID dose was comparable to 10 mg/kg baricitinib BID (Figure 5B). To corroborate this finding in a second model, a keyhole limpet hemocyanin (KLH) delayed type hypersensitivity mouse study was performed. BALB/c mice were immunised subcutaneously with KLH/Complete Freund's Adjuvant on day 0 and then challenged in the ear subcutaneously with KLH on day 7. 10 mg/kg baricitinib or SYX-PKM-A were administered in single oral doses 1 hour prior to the day 7 KLH challenge. This resulted in a dose dependent decrease in ear thickness 24 hours after the challenge (Figure 5C). SYX-PKM-A caused a decrease in ear thickness at the 10 mg/kg dose that was comparable to baricitinib.

These studies indicated that PKM2 modulators may be efficacious in inflammatory diseases with high serine demand, such as AD.

PKM2 modulation inhibits T cell function in a mouse chronic house dust mite model

The mouse chronic house dust mite model was selected as a well characterised system with a robust Th2 driven immune response to explore the immunological impact of SYX-PKM-A in inflammation [46,47]. 25 µg house dust mite allergen was delivered intranasally to BALB/c mice four times per week for five weeks, with measurement of airway dynamics, bronchoalveolar lavage fluid (BALF) cytokines and BALF cells on day 32 (Supplementary Figure 4A). A recombinant anti-mouse IL-13-mIgG1 antibody was dosed subcutaneously at 10 mg/kg once per week as a reference control. SYX-PKM-A and baricitinib were administered orally BID throughout the model at the doses indicated. Body weight was unaffected by SYX-PKM-A treatment (Supplementary Figure 3A). SYX-PKM-A resulted in a dose-dependent decrease in HDM driven airway resistance with a corresponding increase in dynamic compliance in response to methacholine challenge (Supplementary Figure 4B and 4C). These phenotypes were associated with

observed decreases in lymphocytes, eosinophils and neutrophils (Supplementary Figure 4D, 6E and 6F). SYX-PKM-A did not decrease BALF macrophages, whereas a decrease was observed with anti-IL-13 treatment (Supplementary Figure 4G). The PKM-SYX-A driven decrease in lymphocytes correlated with dose-dependent decreases in the activated T cell cytokines, IL-4, IL-13, IL-5 and RANTES (Supplementary Figure 4H - K). The impact on these readouts were mostly comparable between 100 mg/kg SYX-PKM-A and baricitinib. The effects of 300 mg/kg SYX-PKM-A were more comparable with anti-IL-13. These results support the hypothesis that PKM2 modulation will inhibit the function of multiple T cell subsets in inflammatory disease.

PKM2 upregulation and high serine demand provide an environment for tissue targeted efficacy of PKM2 modulators in AD

The tissue microenvironment is poorly characterised in inflammatory diseases such as AD. Two studies revealed a decrease in L-serine in AD stratum corneum tape strips compared to healthy [48,49]. Other metabolomic studies have been conducted on biopsies from AD skin but did not measure serine and had limited characterisation of the intermediates of glycolysis and nucleotide metabolism [50,51]. Similar to the tape strip studies, serine was found to be decreased in AD biopsies compared to healthy (Figure 5D). This was associated with increases in many purine and pyrimidine metabolism pathway metabolites, consistent with increased serine demand in AD (Figure 5E). PKM gene expression was significantly increased in AD tape strips from a previously published study [52] and trended towards a significant increase in a second study [53] (Figure 5F). In confirmation of this finding, elevated PKM2 protein was also observed in severe AD biopsies (Figure 5G). Expression of one carbon metabolism, plasma membrane serine transporter and nucleotide metabolism genes was also increased in AD tape strips compared to healthy (Figure 5H; Supplementary Figure 3B). These data revealed AD as a disease with elevation of PKM2 and high serine demand, which is an environment for potential tissue targeted efficacy of PKM2 modulators.

Discussion

Previous studies reveal a disconnect between the *in vitro* potency of TEPP-46 in T cells and efficacy in animal models of inflammation or autoimmunity [5–7,34–36]. This study identifies serine demand as a factor responsible for this disconnect and the key determinant of the cellular and tissue-level response to PKM2 modulation. TEPP-46 is a tool compound that has not entered clinical trials. Therefore SYX-PKM-A was developed as a PKM2 modulator with suitable physiochemical, ADME and pharmacokinetic properties for oral treatment of inflammatory diseases. SYX-PKM-A converts PKM2 to tetrameric form, resulting in increased pyruvate kinase activity. SYX-PKM-A restricts flux through serine biosynthesis in human lymphocytes, leading to inhibition of proliferation, cytokine production and antibody secretion under conditions of high serine demand without affecting viability. In support of this hypothesis, these

phenotypes are rescued by addition of exogenous formate. The cellular compensatory response to this reduction in metabolically available serine is to upregulate expression of serine biosynthesis, plasma membrane serine transporters, one carbon metabolism and nucleotide metabolism pathways to maintain nucleotide and protein synthesis. Importantly, this conditional metabolic vulnerability dependent on serine demand is present in human atopic dermatitis (AD) skin and is recapitulated in multiple mouse models of inflammation. This establishes a tissue-targeted therapeutic opportunity for PKM2 modulation in inflammatory disease (Fig. 6).

PKM2 activators such as TEPP-46 have previously been shown to divert glycolytic flux away from 3-phosphoglycerate-derived serine biosynthesis in A549 lung adenocarcinoma, H460 large cell lung carcinoma and MDA-MB-468 breast adenocarcinoma cells [12,13]. However, this phenotype was absent in SW480 colorectal adenocarcinoma and H522 lung adenocarcinoma cells, suggesting that this finding is not universally applicable to all cancer types. In contrast, SYX-PKM-A inhibited proliferation and function in all tested lymphocytes, including human IgG-releasing B cells, IgE-releasing B cells, CD4 + T cells, Th2 cells, Th17 cells and IFNγ releasing PBMCs stimulated with Td-IPV. This reinforces findings of a common requirement for serine to fuel one carbon metabolism and downstream protein synthesis and nucleotide biosynthesis in T and B cells [16–20]. At concentrations of TEPP-46 that can't be achieved *in vivo*, PKM2 is converted to tetrameric form in stimulated mouse CD8 + T cells, CD4 + T cells, Th1 and Th17 cells, blocking proliferation and cytokine release [5–7,14]. However, this study provides a more robust link between *in vitro* effects of PKM2 modulation on inflammatory lymphocytes at nanomolar concentrations under conditions of high serine demand, which is more representative of the tissue microenvironment in inflammatory skin disease compared to standard media.

T cell activation following immune challenge results in a high level of glycolysis to support clonal expansion and serine is critical for this response [16]. In the Ma *et al.* study, mice fed a serine/glycine free diet had a limited T cell response to OVA-expressing Listeria monocytogenes infection with a 50% reduction in IFNγ producing CD8 + T cells. Interestingly the quantity of cytokine produced per cell was unaffected by diet. This supports the conclusion that PKM2 modulation in low serine media inhibits proliferation and that cytokine release is reduced as a result, rather than a direct PKM2-mediated effect on cytokine release. Similarly, the SYX-PKM-A mediated reduction in BALF lymphocytes in the mouse chronic house dust mite model correlated with a reduction in cytokines, consistent with a reduction in lymphocyte proliferation. This is a Th2 driven model with aspects of epithelial cell damage and activity of dendritic cells, mast cells, eosinophils, basophils and ILC2s [46,47]. Therefore, it is possible that PKM2 modulation impacts multiple inflammatory cell types in this model including an anti-proliferative effect on lymphocytes.

In contrast to T cells, the key impact of PKM2 modulation in B cells is not anti-proliferative, rather it is mediated via serine as an amino acid precursor of glycine, cysteine and methionine to support antibody synthesis. This is concordant with the metabolic reprogramming of B cells that occurs upon activation, with an increase in glycolysis to support antibody production [54]. In IgG-polarising conditions, SYX-PKM-A

reduced IgG release and plasmablast frequency in low serine media. In contrast, IgE secretion was inhibited without loss of plasmablasts, consistent with evidence that IgE production is less tightly coupled to acquisition of a canonical plasmablast phenotype and can arise from phenotypically heterogeneous antibody-secreting cells [55,56]. Although antibody-secreting B cell responses are reduced in response to SYX-PKM-A, memory B cells are maintained, suggesting that vaccine responses would remain intact in patients treated with a PKM2 modulator. This profile is beneficial compared to broad spectrum systemic immunosuppressive agents such as methotrexate, which impair vaccine response [57].

This study has implications for future drug development efforts. Classical cell culture media maintain cells in non-physiologic nutrient conditions that can distort metabolism, signalling and drug responses [58]. In human plasma-like media, T cell activation and transcriptomic profile are altered compared to culture in traditional RPMI media, demonstrating that appropriate *in vitro* culture conditions should be considered to accurately model patient responses to therapy [59]. However, the metabolite profile in plasma is not representative of the tissue microenvironment in which T cells perform effector functions in inflammatory diseases such as AD [48,50,51]. Disease tissue microenvironment is better emulated in animal models compared to *in vitro* systems and serine is the most downregulated metabolite in inflamed ears in the T-cell-driven trinitrochlorobenzene (TNCB) hapten model, which is similar to the DNFB model [60]. This aligns with the reduction in serine observed in the DNFB model in this study. However, animal models do not completely recapitulate human disease [45] and our study demonstrates how local metabolite demand in disease can dictate responsiveness to treatment. Therefore, there is a need for more extensive profiling of inflammatory tissue and more disease appropriate *in vitro* culture systems to study cellular treatment responses. For example, a meta-analysis is required to define an AD skin metabolome and guide physiological media composition for development of novel AD therapeutics with low healthy tissue toxicity.

JAK inhibitors including baricitinib have good efficacy in AD but are generally reserved for use in patients for whom other systemic therapies have failed, due to their risk-benefit profile. SYX-PKM-A was at least as efficacious as JAK inhibition in 3 different mouse models of inflammation, suggesting that PKM2 modulation could be a valuable treatment option for AD patients. IL-4/IL-13 biologics are approved for AD treatment and SYX-PKM-A had comparable efficacy to an anti-IL-13 mAb in many chronic house dust mite model readouts. The availability of a safe oral treatment such as a PKM2 modulator would be particularly important in diseases such as AD which has a prevalence of 10–20% in the paediatric population in Europe and the USA, for which treatment safety is paramount [27,28]. Accordingly, the PKM2 modulator, SYX-5219, has recently entered clinical trials in healthy volunteers and AD patients.

High serine demand has been described in other inflammatory diseases such as psoriasis, Crohn's disease, ulcerative colitis and rheumatoid arthritis [22,23]. However, further studies will be required to determine if high PKM2 expression and coincident high serine demand are characteristics particular to AD, or whether similar environments are present in other inflammatory diseases. This will be invaluable to determine if PKM2 modulation may be efficacious in indications other than AD. The current study has

defined a gene signature that could be used to address this question. Further work is also required to elucidate the relative contribution of canonical and non-canonical PKM2 functions in animal models of inflammation as determinants of PKM2 modulator efficacy [1,4]. This study highlights the potential for tissue-restricted immunomodulation of a PKM2 modulator at AD inflammatory sites, enabling a differentiated safety profile. Ultimately clinical trials are required to study safety and efficacy of PKM2 modulation in patients. The ongoing oral SYX-5219 PKM2 modulator clinical trial in AD patients may provide support for this approach, with the potential to rebalance immune function and drive sustained disease remission. This PKM2 modulator could address the major unmet needs of AD where there are limited treatment options under the current standard of care.

Methods

Chemistry

SYX-PKM-A was synthesised as described in the Supplementary Experimental Procedures.

PKM2 Enzyme assays

Recombinant human PKM2 (Bio-Techne, 7244-PK-020) and mouse PKM2 (Abcam, ab223006) activity were measured using a 384-well luminescent endpoint assay. Enzymes were diluted in assay buffer (50 mM imidazole pH 7.2, 50 mM KCl, 7 mM $MgCl_2$, 0.01% Tween-20, 0.05% BSA) to final concentrations of 5 pM (human) or 50 pM (mouse) and dispensed into ProxiPlate-384 plates (PerkinElmer, 6008280). Compounds were dispensed acoustically. Following 10 minutes pre-incubation at room temperature, reactions were initiated by addition of phosphoenolpyruvate (PEP; Sigma, 860077-1G) and ADP (2BScientific, ADP100-2) to final concentrations of 53 µM and 219 µM, respectively, and incubated for 60 minutes at 26°C with shaking. Kinase activity was quantified using Kinase-Glo Plus reagent (Promega, V3773), followed by 15 minutes incubation and luminescence detection on a PHERAstar FSX plate reader. Data were normalized to DMSO (low) and 5 µM TEPP-46 (high) controls, and concentration–response curves were fitted using a four-parameter logistic model to determine EC_{50} and Emax values with profile-likelihood confidence intervals.

Cell isolation and culture

Negative selection EasySep Isolation Kits from StemCell Technologies were used to isolate primary human CD4 + T (17952), naïve CD4 + T cells (17555), memory CD4 + T cell (19157) or B cells (17954) from peripheral blood mononuclear cells obtained from leukocyte cones. For functional assays, cells were thawed rapidly, washed, and resuspended in pre-warmed media prior to counting using acridine orange/propidium iodide (VWR, NEXCCS2-0106) staining on a Nexcelom Cellometer. Where required, cells were labelled with CFSE (Invitrogen, C34554) to monitor proliferation. Cells were seeded in 96-well U-bottom plates in RPMI-1640 medium (Thermo Fisher Scientific, 21875091) with 10% heat-inactivated fetal bovine serum (Gibco, 11550356) or serine-free RPMI-1640 medium (Thermo Fisher Scientific) with dialysed FBS (Gibco, 26400044) and 10 µM, 100 µM or 280 µM serine as indicated. Media were

supplemented with 2 mM L-glutamine (Fisher Scientific, 11500626) and penicillin/streptomycin (Merck, P4333). For total CD4 + cell experiments, cells were stimulated for 5 days using anti-CD3/CD28 Dynabeads (Gibco, 10548353). For Th2 experiments, naïve CD4 + T cells were stimulated for 5 days with αCD3/αCD28 beads, αIFNγ (R&D Systems, MAB285-500), IL-2 (PeproTech, 200-02-500UG) and IL-4 (PeproTech, 200-04-20uG). Th17-polarising conditions were established from memory CD4 + T cells using anti-CD3 (OKT3 clone; BD Pharmingen, 566685) and anti-CD28 (BioLegend, 302902) each at 1 µg/mL, in combination with cytokines IL-1β (R&D Systems, 201-LB-010) and IL-23 (R&D Systems, 1290-IL-010) at 50 ng/mL, IL-2 at 50 IU/mL, and neutralising antibodies against IFNγ and IL-4 (PeproTech, 500702) each at 1 µg/mL for 6 days. PBMCs were stimulated with Td-IPV (Baymed Healthcare, VARE001) and IL-2 for 13 days. CD19 + B cells were activated using B cell receptor crosslinking with anti-IgG/IgM (Jackson ImmunoResearch, 309-005-003), CD40 ligation with MegaCD40L (Enzo Life Sciences, ALX-522-110-C010), and cytokines including IL-21 (PeproTech, 200-21-100UG), IL-2, IL-4 and IL-13 (PeproTech, 200-13-100UG) included where required to drive class-switching responses as described in the results.

A549 cells (Merck, 86012804) were seeded into 96-well plates at 5–10 × 10^3 cells per well in serine free Basal Medium Eagle (Thermo Fisher Scientific, 21010046) supplemented with 10% fetal bovine serum, 1% penicillin/streptomycin and 20 µM L-serine (Sigma, S4311) under standard culture conditions (37°C, 5% CO_2). Cells were incubated with compound for 72 hours and cell viability was quantified using an CellTiter-Glo ATP-based luminescence assay (Promega, G9241), according to the manufacturer's instructions, with luminescence measured on a Pherastar FSX plate reader (BMG Labtech) and normalised to vehicle-treated controls.

After plating cells and addition of stimuli, compounds were prepared as 10 mM or 20 mM DMSO stocks and dispensed using either an Echo 550/650 acoustic liquid handler (Beckman Coulter Life Sciences) or D300 liquid dispenser (Tecan). Cells were incubated with compounds for the duration of the assays.

Pyruvate kinase assay

CD4 + T-cells were isolated from leukocyte cones (NHS NCI) by Ficoll-Paque PLUS (Cytiva, 17-1440-02) density centrifugation followed by negative selection using the EasySep human CD4 + T-cell isolation kit (StemCell Technologies, 17952) and cultured in RPMI-1640 medium (Fisher, 11835063) supplemented with 10% heat-inactivated FBS (Sigma, F9665), penicillin/streptomycin (Sigma, P4333) and L-glutamine (Sigma, G7513). Cryopreserved cells were thawed, seeded at 1 × 10^4 cells per well, and treated with compound, DMSO, SYX-PKM-A or TEPP-46 (MedChemExpress, HY-18657) dispensed acoustically for 20 minutes at 37°C, 5% CO_2. Following treatment, cells were washed with medium and PBS, lysed in assay buffer, and clarified lysates were analysed using a pyruvate kinase activity assay kit (Abcam, ab83432). Reaction mixtures were transferred to 384-well plates (Greiner, 781091) and absorbance at 570 nm was measured kinetically using a PHERAstar FSX plate reader. Data were blank-subtracted and normalised to per-plate vehicle (low) and 30 µM TEPP-46 (high) controls, and concentration–response curves were fitted using a four-parameter logistic model to derive EC_{50} and Emax values with profile-likelihood confidence intervals.

DSS crosslinking and western blotting

Mouse bone marrow derived macrophages were stimulated with 10 ng/mL LPS in DMEM media containing 1% FBS and then treated with 30 μM TEPP-46, 1 μM SYX-PKM-A or DMSO. After 24 hours, cells were washed three times with PBS (pH8) and crosslinking was performed using 500 μM disuccinimidyl suberate (Thermo Fisher Scientific Pierce) in PBS (pH 8.0) for 30 minutes at room temperature. The reaction was quenched by addition of Tris-HCl pH 7.5 to a final concentration of 100 mM. Lysates were analysed by western blotting.

For western blotting, cell pellets were lysed in lysis buffer (Cell Signaling Technology, 9803S) supplemented with 1 mM PMSF and protease inhibitors (Cell Signalling Technology, 5872S), using three freeze–thaw cycles and clarification by centrifugation. Total protein concentration was determined using the Pierce BCA Protein Assay Kit (Thermo Fisher Scientific, 10741395) with absorbance measured at 562 nm, and samples were normalised prior to loading. Lysates were mixed with Bolt 4× LDS sample buffer (Thermo Fisher Scientific, B0007) and reducing agent (Thermo Fisher Scientific, B0009), denatured at 75°C for 10 minutes, and resolved on Bolt 4–12% Bis-Tris Plus gels (Thermo Fisher Scientific, NWC4120BOX) using MOPS running buffer (Thermo Fisher Scientific, B0001). Proteins were transferred to PVDF membranes using the iBlot 2 Gel Transfer Device (Thermo Fisher Scientific, IB24001). Membranes were blocked in Azure fluorescent blocking buffer (Azure Biosystems, AC2190) for 45 minutes at room temperature, washed in TBST/PBST, and incubated overnight at 4°C with primary antibodies against PKM2 (clone D78A4, Cell Signaling Technology, 4053) and β-actin (Cell Signalling Technology, 3700). Following washing, membranes were incubated with fluorescent secondary antibodies (Azure Biosystems, AC2129 and AC2134), washed, and imaged using a Sapphire Biomolecular Imager (Azure Biosystems). PKM2 signal intensity was normalised to β-actin and expressed relative to baseline controls.

Flow cytometry

Cells were washed and stained in flow cytometry buffer consisting of PBS (Life Technologies, 14190250) supplemented with 2% heat-inactivated fetal bovine serum (Gibco/Fisher Scientific, 11550356) and 2 mM EDTA (Life Technologies, 15575020). For extracellular staining, cell pellets were washed in PBS, then incubated for 20 minutes at 4°C in the dark with antibody master mixes prepared in PBS and containing the Fc receptor blocker (Human TruStain FcX, BioLegend, 422302), Live/Dead Fixable viability dye (Thermo Fisher Scientific), and, where multiple Brilliant Violet fluorophores were used, Brilliant Buffer Plus (BD Biosciences, 566385). Cells were washed, then fixed in BD Cytofix Fixation Buffer or fixed and permeabilized using the eBioscience Foxp3/Transcription Factor Staining Buffer Set (Thermo Fisher Scientific, 00-5523-00). For intracellular staining, cells were then incubated with intracellular antibody mixes in permeabilization buffer, washed, and resuspended in flow buffer for acquisition. Compensation controls were prepared using UltraComp eBeads (Invitrogen, 01-2222-41) for antibody fluorophores and ArC Amine Reactive Compensation Beads (Invitrogen, A10628) for Live/Dead dyes. Fluorescence-minus-one and isotype controls were included as appropriate. Samples were acquired on an Attune flow

cytometer (Thermo Fisher Scientific). Data was analysed using FlowJo™ v10.10 Software. Division index was calculated using the proliferation modelling tool, with the unstimulated control cells serving as peak 0 non-proliferated. Plasmablasts were identified by gating live cells which were CD20- CD27 + CD38+ CD138-. Memory B cells were identified by gating live CD38- CD20 + CD27+.

Metabolite measurement and flux analysis

Polar metabolite profiling and isotope-tracing analyses were performed on extracts from primary human CD4 + T cells. CD4 + T cells were stimulated with αCD3/αCD28 beads for 3 days in media containing 10 μM serine. 4 mM heavy labelled α-15N L-glutamine (Cambridge Isotope Laboratories, NLM-1016-0.1) was added for the final 4 hours (phosphoserine measurement) or 24 hours (ATP measurement) in glutamine-free media. Cells were pooled across replicate wells, centrifuged, washed once with freshly prepared 75 mM ammonium carbonate buffer (pH 7.3–7.5), and re-pelleted prior to metabolite extraction. Metabolism was quenched by addition of cold (− 20°C) extraction solvent (acetonitrile:methanol:water, 4:4:2), followed by two sequential extraction steps with centrifugation, pooling of supernatants, and storage of clarified extracts at − 80°C. Cell extracts were analysed using targeted polar LC–MS/MS for absolute serine quantification. Untargeted metabolomics was performed using a high-throughput platform in negative ion mode, with pooled study samples injected periodically for quality control and metabolite annotation performed against HMDB, KEGG and ChEBI databases. Targeted isotopologue analysis focused on phosphoserine and ATP to assess propagation of the 15N label through serine biosynthesis and de novo purine synthesis pathways. Extracellular formate levels were quantified in Th2 cell culture supernatants using a colourimetric Formate Assay Kit (Abcam, ab111748), in which formate is enzymatically oxidised to generate a chromogenic product detected at 450 nm. Samples (5 μL) and standards were incubated with equal volumes of reaction mix for 1 hour at 37°C in 384-well plates, and absorbance was measured using a PHERAstar FSX plate reader (BMG Labtech) to interpolate concentrations from a standard curve.

RNA extraction and qPCR

RNA was extracted from human Th2 cells using the Quick-RNA 96 Kit (Zymo Research; Cambridge Bioscience, R1052 and R1053) according to the manufacturer's protocol. 1×10^5 cells per well were lysed directly in 96-well plates with 100 μL RNA lysis buffer and stored at − 80°C prior to processing. On the day of extraction, lysates were thawed to room temperature, mixed 1:1 with ethanol (Merck Life Science, 32205-2.5L-M), and transferred to Silicon-A binding plates for centrifugation at 2,500 × g. Following on-column DNase I digestion, samples were washed sequentially with RNA prep and wash buffers and eluted in 25 μL nuclease-free water (Life Technologies, AM9939). RNA concentration and purity were determined using a Nanodrop (Thermo Fisher Scientific), and samples were normalised prior to downstream applications. Complementary DNA (cDNA) was synthesised from purified RNA using the Maxima First Strand cDNA Synthesis Kit (Thermo Fisher Scientific, K1642 or K1672) following incubation at 25°C (10 minutes), 50°C (15 minutes), and 85°C (5 minutes), and subsequently diluted prior to use. Quantitative PCR was performed using TaqMan Fast Advanced Master Mix (Applied Biosystems, 4444963) with TaqMan gene expression assays (FAM and VIC-labelled; Applied Biosystems, 4331182,

4351368, 4448508) in 96- or 384-well optical plates. Reactions were run on a QuantStudio 6 Flex Real-Time PCR system (Applied Biosystems) using standard cycling conditions (50°C 2 minutes, 95°C 20 seconds, followed by 40 cycles of 95°C for 1 second and 60°C for 20 seconds). Gene expression was quantified using the comparative Ct (2^−ΔΔCt) method, normalising target gene expression to an endogenous control and expressing fold changes relative to control samples.

Measurement of secreted analytes

Homogeneous time-resolved fluorescence (HTRF) or Meso Scale Discovery (MSD) immunoassays were performed to measure analytes in cell culture supernatants according to protocols. For HTRF assays, cell culture supernatants were thawed, clarified by centrifugation and transferred to white 384-well plates (Greiner Bio-One, 784075), with 8 µL sample combined with 2 µL detection antibody mix. HTRF kits were from Revvity (IFNγ 62HIFNGPEH, IgG 6FHIGPEG, IL-17A 62HIL17PEH), and antibodies were combined directly at 1:40 dilution in detection buffer immediately before addition to the plate. Plates were read on a PHERAstar FSX plate reader (BMG Labtech), and data were analysed in BMG MARS software with HTRF ratio calculated as 665 nm/620 nm × 10,000 and concentrations interpolated from 4-parameter logistic standard curves. For MSD assays, supernatants were analysed using MSD kits (IL-13 K151UBK, IL-31 K151WEK, IgE K1515AR) on 96-well plates read on an MSD Sector Imager S120 instrument. Assays were performed using manufacturer-supplied diluents, wash steps used filtered PBS/0.05% Tween-20, and plate washing was performed using a Multidrop Combi dispenser with manual buffer removal (Thermo Fisher Scientific). Plates were incubated with standards and samples according to kit-specific instructions, read after addition of MSD read buffer, and analysed in MSD Discovery Workbench software.

Analytes in the BALF were quantified with a Luminex kit using the Magpix instrument according to the manufacturer instructions (Biotechne, FCSTM20).

Animal models

Pharmacokinetics of TEPP-46 and SYX-PKM-A were assessed following a single PO dose of 60 mg/kg SYX-PKM-A or 3 mg/kg TEPP-46 in male C57BL/6 mice.

For the DNFB model, female BALB/c mice (6–8 weeks) were sensitised by topical application of 1% DNFB (Sigma, D1529) in acetone/olive oil (4:1) to the abdomen on days 0 and 1, followed by ear challenge with 0.5% DNFB on day 5. Mice were treated with a single dose of 10 mg/kg baricitinib PO, or SYX-PKM-A at 1 mg/kg, 3 mg/kg, 10 mg/kg or 30 mg/kg PO at 1 hour prior to the challenge.

For the keyhole limpet hemocyanin (KLH) immunisation model, female BALB/c mice (8 weeks) were immunised on day 0 with 100 µL of an emulsion comprising keyhole limpet hemocyanin (KLH Sigma, H7017; 4 mg/mL in 0.9% NaCl) mixed 1:1 with complete Freund's adjuvant containing *Mycobacterium butyricum* (BD Biosciences, 263810; 0.5 mg/mL) in paraffin oil with emulsifier. On day 7, animals were challenged by intradermal injection of 20 µL KLH solution (4 mg/mL) into the left ear, while the contralateral ear received vehicle control (0.9% NaCl). Mice were treated with a single dose of 10 mg/kg

baricitinib PO, or SYX-PKM-A at 1 mg/kg, 10 mg/kg, 30 mg/kg, 60 mg/kg or 100 mg/kg PO at 1 hour prior to the challenge. Ear thickness measured 24 hours after challenge using calipers for both the DNFB and KLH models.

For the chronic house dust mite (HDM) asthma model, female BALB/c mice were sensitised intranasally with HDM extract (25 µg; Stallergenes Greer, XPB91D3A2.5) for 4 consecutive days per week over 5 weeks. Animals were treated twice daily (p.o., 10 mL/kg) with SYX-PKM-A (10–300 mg/kg), 10 mg/kg baricitinib or vehicle, while anti-IL-13 antibody (InvivoGen, mil13-mab9) was administered weekly by subcutaneous injection. Airway hyper-responsiveness was assessed 24 h after the final challenge by methacholine provocation using whole-body plethysmography (DSI FinePointe), and bronchoalveolar lavage fluid was collected for differential cell counts and cytokine analysis using Luminex assays.

The vehicle used for these studies was 1% hydroxypropyl methylcellulose (Sigma, H7509), 0.25% Tween 80 (Damas, 89191C) and 0.005% simethicone (Sigma, 1612652).

Immunohistochemistry

PKM2 expression in AD skin biopsies was assessed by chromogenic immunohistochemistry on formalin-fixed, paraffin-embedded human skin punch biopsies. Serial 4 µm sections were cut and transferred onto SuperFrost Plus slides. Prior to staining, slides were baked at 60°C, dewaxed, rehydrated, and subjected to heat-induced epitope retrieval in citrate-based low-pH antigen unmasking solution (Vector Laboratories, H-3300) using a pressure cooker for 4 minutes, followed by cooling for 10 minutes. After washing, sections were blocked with normal horse serum from the ImmPRESS AP Horse Anti-Rabbit IgG Polymer Detection Kit (Vector Laboratories, MP-5401) and incubated for 60 minutes at room temperature with anti-PKM2 rabbit monoclonal antibody (D78A4, Cell Signaling Technology, 4053S) at 1:400 dilution in PBS containing 0.1% Tween-20 (Sigma-Aldrich, P1379). Antibody binding was detected using the ImmPRESS alkaline phosphatase polymer system (Vector Laboratories, MP-5401), followed by development with Liquid Permanent Red substrate (Agilent, K0640) containing levamisole (Vector Laboratories, SP-5000-18) to suppress endogenous alkaline phosphatase activity. Slides were counterstained with Mayer’s haematoxylin (Pioneer Research Chemicals, PRC/R/42), dehydrated, cleared, and mounted with EcoMount (CellPath, PBC-BRR897L). Whole-slide brightfield images were acquired at 20× magnification on a Hamamatsu NanoZoomer S360 and analysed in Visiopharm to quantify PKM2-positive cells and staining intensity across epidermal, dermal, and glandular/subcutaneous regions.

Declarations

Animal ethics statement:

All animal experiments were performed in accordance with relevant institutional and national regulations and guidelines and were approved before commencement by the appropriate institutional and/or licensing authorities. The single-dose pharmacokinetic study and the DNFB models were conducted at

Shanghai ChemPartner Co., Ltd., People's Republic of China, in accordance with the Regulations for the Administration of Affairs Concerning Experimental Animals, as amended on 1 March 2017. The animal care and use programme at the facility was accredited by AAALAC International at the time the studies were performed. The experimental protocols were reviewed and approved by the ChemPartner Institutional Animal Care and Use Committee under protocol numbers CPB-P25-66236M02 (single-dose pharmacokinetic study), CPB-P24-28910 (DNFB model 1), and CPB-P22-26640 (DNFB model 2). The KLH model was conducted at Selvita Ltd., Croatia, in accordance with Directive 2010/63/EU and the Croatian Ordinance on the Protection of Animals Used for Scientific Purposes (Official Gazette Nos. 55/13, 39/17 and 116/19). The animal care and use programme at the facility was accredited by AAALAC International at the time of the study. The protocol was reviewed and approved before commencement by Selvita's Committee for Research Animal Ethics under approval number SP-278-22. The chronic house dust mite model was conducted at Pharmidex Pharmaceutical Services UK in accordance with the UK Animals (Scientific Procedures) Act 1986, as amended, under UK Home Office Project Licence PP0969406. The work underwent local ethical review by the Pharmidex Animal Welfare and Ethical Review Body.

Acknowledgements

Study conception, data interpretation, and manuscript writing were performed by the listed authors. Experimental execution included external technical support as follows: SYX-PKM-A was developed under a license agreement with Eli Lilly. Sygnature generated the data in the recombinant enzyme assays, CD4 + T cell pyruvate kinase assays and A549 assays. Metabolomics and flux analysis data was generated at Clinical Microbiomics and General Metabolics with AD skin biopsies provided by Cureline. PKM2 IHC was completed at Histologix. The mouse DNFB, KLH and chronic house dust mite studies were performed at ChemPartner, Selvita and Pharmidex, respectively.

References

1. Lee Y et al (2022) Multiple functions of pyruvate kinase M2 in various cell types. J Cell Physiol 237:128–148
2. Nandi S, Dey M (2020) Biochemical and structural insights into how amino acids regulate pyruvate kinase muscle isoform 2. J Biol Chem 295:5390–5403
3. Dombrauckas JD, Santarsiero BD, Mesecar AD (2005) Structural Basis for Tumor Pyruvate Kinase M2 Allosteric Regulation and Catalysis †, ‡. Biochemistry 44:9417–9429
4. Pålsson-McDermott EM, O'Neill LA (2020) J. Targeting immunometabolism as an anti-inflammatory strategy. Cell Res 30:300–314
5. Angiari S et al (2020) Pharmacological Activation of Pyruvate Kinase M2 Inhibits CD4 + T Cell Pathogenicity and Suppresses Autoimmunity. Cell Metab 31:391–405e8
6. Seki SM et al (2020) Modulation of PKM activity affects the differentiation of TH17 cells. Sci Signal 13

7. Chen C et al (2022) Vitamin B5 rewires Th17 cell metabolism via impeding PKM2 nuclear translocation. Cell Rep 41:111741
8. Subleski JJ et al (2026) Pyruvate kinase muscle 2 (PKM2) promotes CD4 T cell survival by regulating pyruvate oxidation during homeostasis and expansion. Sci Adv 12:eaec5092
9. Deng J et al (2017) Homocysteine Activates B Cells via Regulating PKM2-Dependent Metabolic Reprogramming. J Immunol 198:170–183
10. Zhou L et al (2021) NEK2 Promotes Cell Proliferation and Glycolysis by Regulating PKM2 Abundance via Phosphorylation in Diffuse Large B-Cell Lymphoma. Front Oncol 11:677763
11. Bagaloni I et al (2021) Metabolic Switch and Cytotoxic Effect of Metformin on Burkitt Lymphoma. Front Oncol 11:661102
12. Kung C et al (2012) Small Molecule Activation of PKM2 in Cancer Cells Induces Serine Auxotrophy. Chem Biol 19:1187–1198
13. Benzarti M et al (2024) PKM2 diverts glycolytic flux in dependence on mitochondrial one-carbon cycle. Cell Rep 43:113868
14. Farsani SSM et al (2025) Pyruvate kinase M2 activation reprograms mitochondria in CD8 T cells, enhancing effector functions and efficacy of anti-PD1 therapy. Cell Metab. 10.1016/j.cmet.2025.03.003
15. Meiser J et al (2016) Serine one-carbon catabolism with formate overflow. Sci Adv 2:e1601273
16. Ma EH et al (2017) Serine Is an Essential Metabolite for Effector T Cell Expansion. Cell Metab 25:345–357
17. D'Avola A et al (2022) PHGDH is required for germinal center formation and is a therapeutic target in MYC-driven lymphoma. J Clin Invest 132
18. Kurniawan H et al (2020) Glutathione Restricts Serine Metabolism to Preserve Regulatory T Cell Function. Cell Metab 31:920–936e7
19. Ron-Harel N et al (2016) Mitochondrial Biogenesis and Proteome Remodeling Promote One-Carbon Metabolism for T Cell Activation. Cell Metab 24:104–117
20. Wu J et al (2024) Metabolic determinants of germinal center B cell formation and responses. Nat Chem Biol 1–12. 10.1038/s41589-024-01690-6
21. Novak JSS et al (2025) The integrated stress response fine-tunes stem cell fate decisions upon serine deprivation and tissue injury. Cell Metab. 10.1016/j.cmet.2025.05.010
22. Cappello A et al (2022) Extracellular serine empowers epidermal proliferation and psoriasis-like symptoms. Sci Adv 8:eabm7902
23. Bai J et al (2019) Identification of a natural inhibitor of methionine adenosyltransferase 2A regulating one-carbon metabolism in keratinocytes. EBioMedicine 39:575–590
24. Bai JDK et al (2024) Serine Supports Epithelial and Immune Cell Function in Colitis. Am J Pathol 194:927–940

25. He M et al (2019) Role of amino acids in rheumatoid arthritis studied by metabolomics. Int J Rheum Dis 22:38–46
26. Hur B et al (2021) Plasma Metabolomic Profiling in Patients with Rheumatoid Arthritis Identifies Biochemical Features Predictive of Quantitative Disease Activity. *medRxiv* 2020.09.13.20193664 10.1101/2020.09.13.20193664
27. Guttman-Yassky E, Renert-Yuval Y, Brunner PM (2025) Atopic dermatitis. Lancet 405:583–596
28. Bieber T (2022) Atopic dermatitis: an expanding therapeutic pipeline for a complex disease. Nat Rev Drug Discov 21:21–40
29. Beck LA et al (2022) Type 2 Inflammation Contributes to Skin Barrier Dysfunction in Atopic Dermatitis. JID Innov 2:100131
30. Anastasiou D et al (2012) Pyruvate kinase M2 activators promote tetramer formation and suppress tumorigenesis. Nat Chem Biol 8:839–847
31. Jiang J et al (2010) Evaluation of thieno[3,2-b]pyrrole[3,2-d]pyridazinones as activators of the tumor cell specific M2 isoform of pyruvate kinase. Bioorg Med Chem Lett 20:3387–3393
32. Barba O, Cousin D (2022) Phthalazine Derivatives as Pyruvate Kinase Modulators
33. Morgan HP et al (2013) M2 pyruvate kinase provides a mechanism for nutrient sensing and regulation of cell proliferation. *Proc. Natl. Acad. Sci.* 110, 5881–5886
34. Palsson-McDermott EM et al (2015) Pyruvate Kinase M2 Regulates Hif-1α Activity and IL-1β Induction and Is a Critical Determinant of the Warburg Effect in LPS-Activated Macrophages. Cell Metab 21:65–80
35. Damasceno LEA et al (2020) PKM2 promotes Th17 cell differentiation and autoimmune inflammation by fine-tuning STAT3 activation. J Exp Med 217
36. Pålsson-McDermott EM, O'Neill LA (2020) J. Targeting immunometabolism as an anti-inflammatory strategy. Cell Res 30:300–314
37. Cantor JR (2019) The Rise of Physiologic Media. Trends Cell Biol 29:854–861
38. Chaneton B et al (2012) Serine is a natural ligand and allosteric activator of pyruvate kinase M2. Nature 491:458–462
39. Yuan M et al (2018) An allostatic mechanism for M2 pyruvate kinase as an amino-acid sensor. Biochem J 475:BCJ20180171
40. Jin C et al (2024) Deciphering the interaction between PKM2 and the built-in thermodynamic properties of the glycolytic pathway in cancer cells. J Biol Chem 300:107648
41. Feng X et al (2017) Rapamycin is highly effective in murine models of immune-mediated bone marrow failure. Haematologica 102:1691–1703
42. Sato M et al (2023) A CCR4 antagonist attenuates atopic dermatitis-like skin inflammation by inhibiting the recruitment and expansion of Th2 cells and Th17 cells. Int Immunol 35:437–446
43. Tapia-Calle G et al (2019) A PBMC-Based System to Assess Human T Cell Responses to Influenza Vaccine Candidates In Vitro. Vaccines 7:181

44. Priest RC et al (2009) Immunomodulatory activity of a methionine aminopeptidase-2 inhibitor on B cell differentiation. Clin Exp Immunol 155:514–522
45. Zhang S et al (2024) Comprehensive analysis of phenotypes and transcriptome characteristics reveal the best atopic dermatitis mouse model induced by MC903. J Dermatol Sci 114:104–114
46. Tomlinson KL, Davies GCG, Sutton DJ, Palframan RT (2010) Neutralisation of Interleukin-13 in Mice Prevents Airway Pathology Caused by Chronic Exposure to House Dust Mite. PLoS ONE 5:e13136
47. Radhouani M, Starkl P (2024) Adjuvant-independent airway sensitization and infection mouse models leading to allergic asthma. Front Allergy 5:1423938
48. Yoshihisa Y et al (2018) Inflammatory cytokine-mediated induction of serine racemase in atopic dermatitis. J Cell Mol Med 22:3133–3138
49. Goleva E et al (2025) Longitudinal integrated proteomic and metabolomic skin changes in patients with atopic dermatitis treated with dupilumab. J Allergy Clin Immunol 155:1536–1546
50. ILVES L et al (2021) Metabolomic Analysis of Skin Biopsies from Patients with Atopic Dermatitis Reveals Hallmarks of Inflammation, Disrupted Barrier Function and Oxidative Stress. Acta Derm - Venereol 101:1052
51. Zhang L, Zeng Y, Sun J (2023) Progress of metabolomics in atopic dermatitis: a systematic review. JDDG: J Dtsch Dermatol Ges 21:229–236
52. Mikhaylov D et al (2021) Transcriptomic Profiling of Tape-Strips From Moderate to Severe Atopic Dermatitis Patients Treated With Dupilumab. Dermatitis 32:S71–S80
53. Duca ED et al (2024) Intrapatient comparison of atopic dermatitis skin transcriptome shows differences between tape-strips and biopsies. Allergy 79:80–92
54. Caro-Maldonado A et al (2014) Metabolic Reprogramming Is Required for Antibody Production That Is Suppressed in Anergic but Exaggerated in Chronically BAFF-Exposed B Cells. J Immunol 192:3626–3636
55. Haniuda K, Fukao S, Kodama T, Hasegawa H, Kitamura D (2016) Autonomous membrane IgE signaling prevents IgE-memory formation. Nat Immunol 17:1109–1117
56. Newman R, Tolar P (2021) Chronic calcium signaling in IgE + B cells limits plasma cell differentiation and survival. Immunity 54:2756–2771e10
57. Kapetanovic MC et al (2017) Methotrexate reduces vaccine-specific immunoglobulin levels but not numbers of circulating antibody-producing B cells in rheumatoid arthritis after vaccination with a conjugate pneumococcal vaccine. Vaccine 35:903–908
58. Cantor JR et al (2017) Physiologic Medium Rewires Cellular Metabolism and Reveals Uric Acid as an Endogenous Inhibitor of UMP Synthase. Cell 169:258–272e17
59. Leney-Greene MA, Boddapati AK, Su HC, Cantor JR, Lenardo MJ (2020) Human Plasma-like Medium Improves T Lymphocyte Activation. *iScience* 23, 100759
60. Zizmare L et al (2022) Acute and chronic inflammation alter immunometabolism in a cutaneous delayed-type hypersensitivity reaction (DTHR) mouse model. Commun Biology 5:1250

Figures

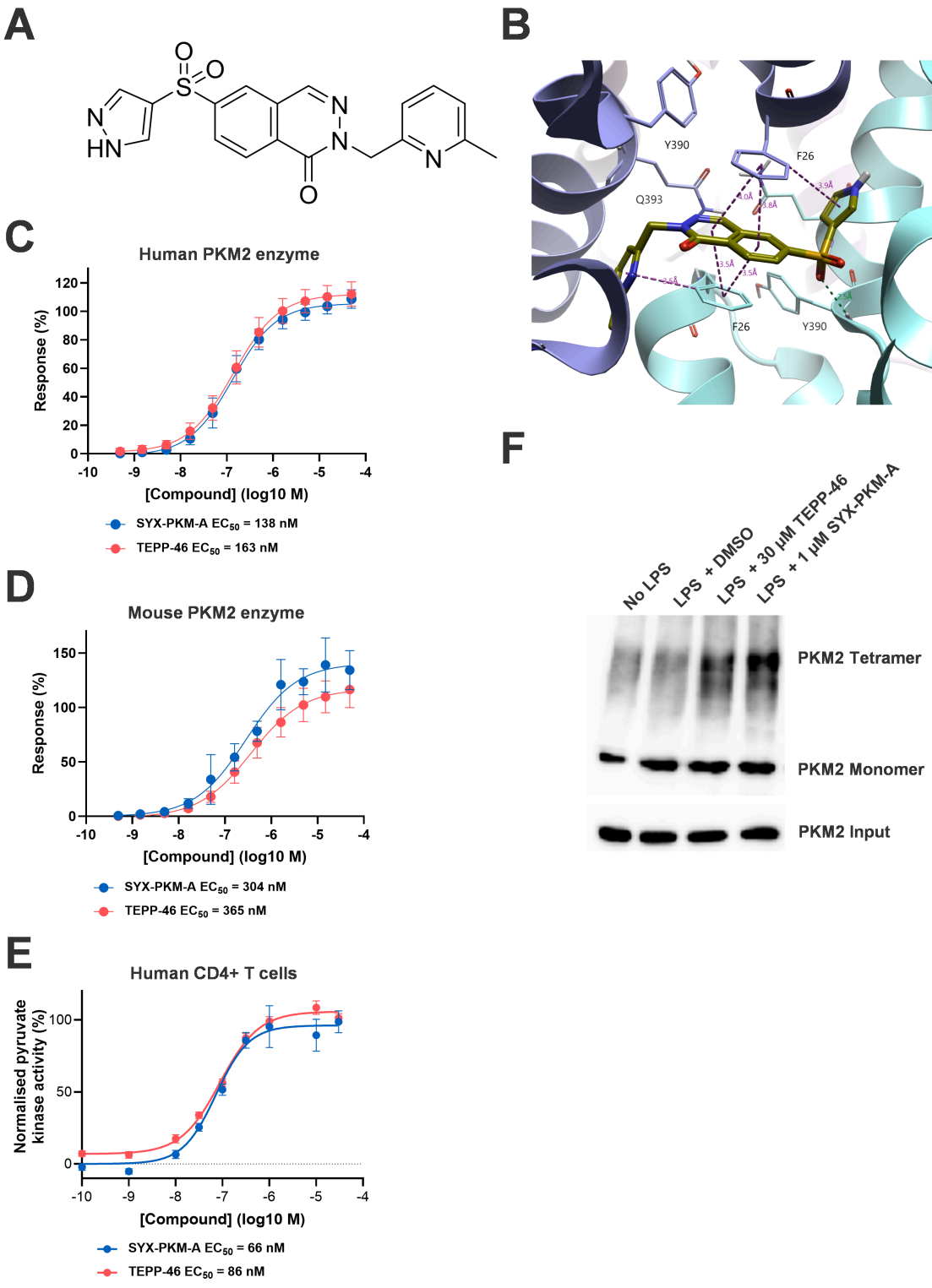


Figure 1

A novel small molecule activates PKM2 in human CD4+ T cells

A. Structure of compound, SYX-PKM-A. B. Docking pose of SYX-PKM-A in the human PKM2 allosteric pocket. Ribbons are coloured by cyan and purple for chains A and B, respectively. SYX-PKM-A is shown as a stick with carbon in green, oxygen in red, nitrogen in blue and sulphur in orange. Key aromatic-aromatic interactions are shown in purple dashed lines and H-bond in green dashed lines. C and D. Activation of recombinant human PKM2 (C) and mouse PKM2 (D). Response data is normalised to plate low (0.65% DMSO vehicle) and high (5 μM TEPP-46) controls. Data are plotted as mean ± SD of at least 4 independent experiments. E. Activation of pyruvate kinase in human CD4+ T cells in standard RPMI media. Response data is normalised to plate low (0.3% DMSO vehicle) and high (30 μM TEPP-46) controls. Data are plotted as mean ± SEM of at least 4 donors. F. PKM2 oligomeric species identified by western blotting using lysates from LPS stimulated mouse bone marrow derived macrophages in standard DMEM media. DSS was used as an amine-reactive crosslinker. PKM2 monomer and tetramer are shown. Data is representative of 3 donors.

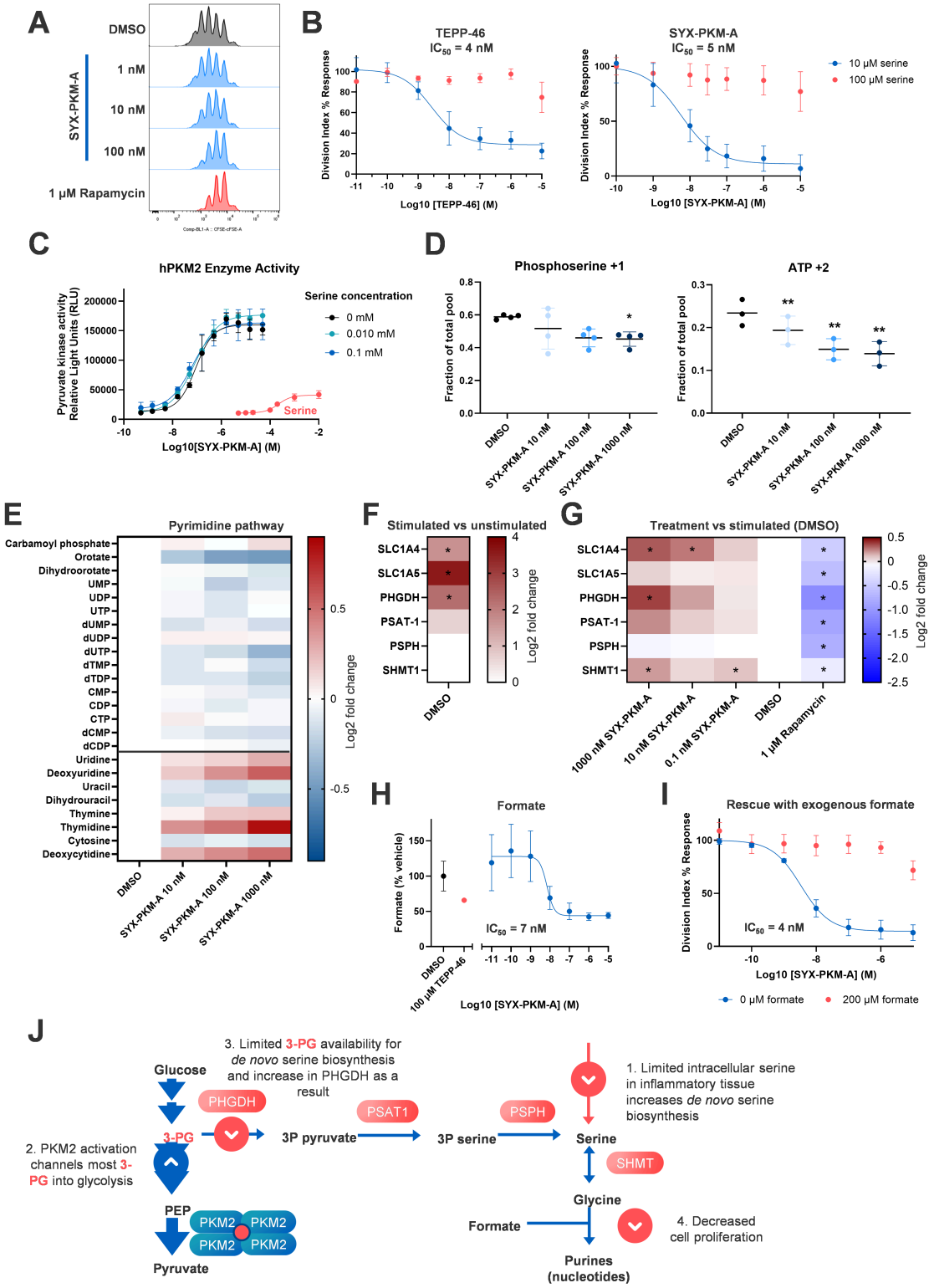


Figure 2

PKM2 activation induces serine auxotrophy in human CD4+ T cells

A. Proliferation of αCD3/αCD28 stimulated human CD4+ T cells after 5 days incubation with SYX-PKM-A in media containing 10 μM serine. 1 μM rapamycin is used as a positive control. Representative donor shown. B. Stimulated CD4+ division index after 5 days incubation with SYX-PKM-A in media containing

either 10 μM or 100 μM serine. Data is presented as % response with normalisation to the DMSO control (100%) and 1 μM rapamycin control (0 %), showing mean ± SEM of 4 donors. C. Activation of recombinant PKM2 by SYX-PKM-A in the presence of 0 mM, 0.01 mM or 0.1 mM serine. A serine titration is also shown in red in the absence of SYX-PKM-A. Data are plotted as mean ± SD of 2 independent experiments. D. Isotopomer tracing with α-15N L-glutamine to study serine synthesis pathway flux. CD4+ T cells were stimulated with αCD3/αCD28 beads for 2 days in media containing 10 μM serine followed by addition of heavy labelled α-15N L-glutamine for 24 hours in glutamine-free media. Label incorporation into phosphoserine +1 and ATP +2 is shown with mean ± SD of 3 donors. One way ANOVA with Dunnett's post-test * $p < 0.05$, ** $p < 0.01$, *** $p < 0.001$, **** $p < 0.0001$. E. Pyrimidine pathway metabolites in CD4+ T cells stimulated with αCD3/αCD28 beads for 3 days in media containing 10 μM serine in the presence of SYX-PKM-A. F and G. Gene expression in Th2 cells cultured in media containing 10 μM serine in the presence of SYX-PKM-A for 3 days. H. Formate release from αCD3/αCD28 stimulated CD4+ T cells after 5 days incubation with SYX-PKM-A or TEPP-46 in media containing 10 μM serine. I. Stimulated CD4+ division index after 5 days incubation with SYX-PKM-A in media containing either 10 μM serine or 10 μM serine and 200 μM formate. J. PKM2 modulation in a high serine demand environment results in decreased flux through the serine biosynthesis pathway. This results in increased expression of serine biosynthesis, serine transporter and one carbon metabolism genes as a compensatory mechanism. The downstream consequence is decreased nucleotide pools and cell proliferation.

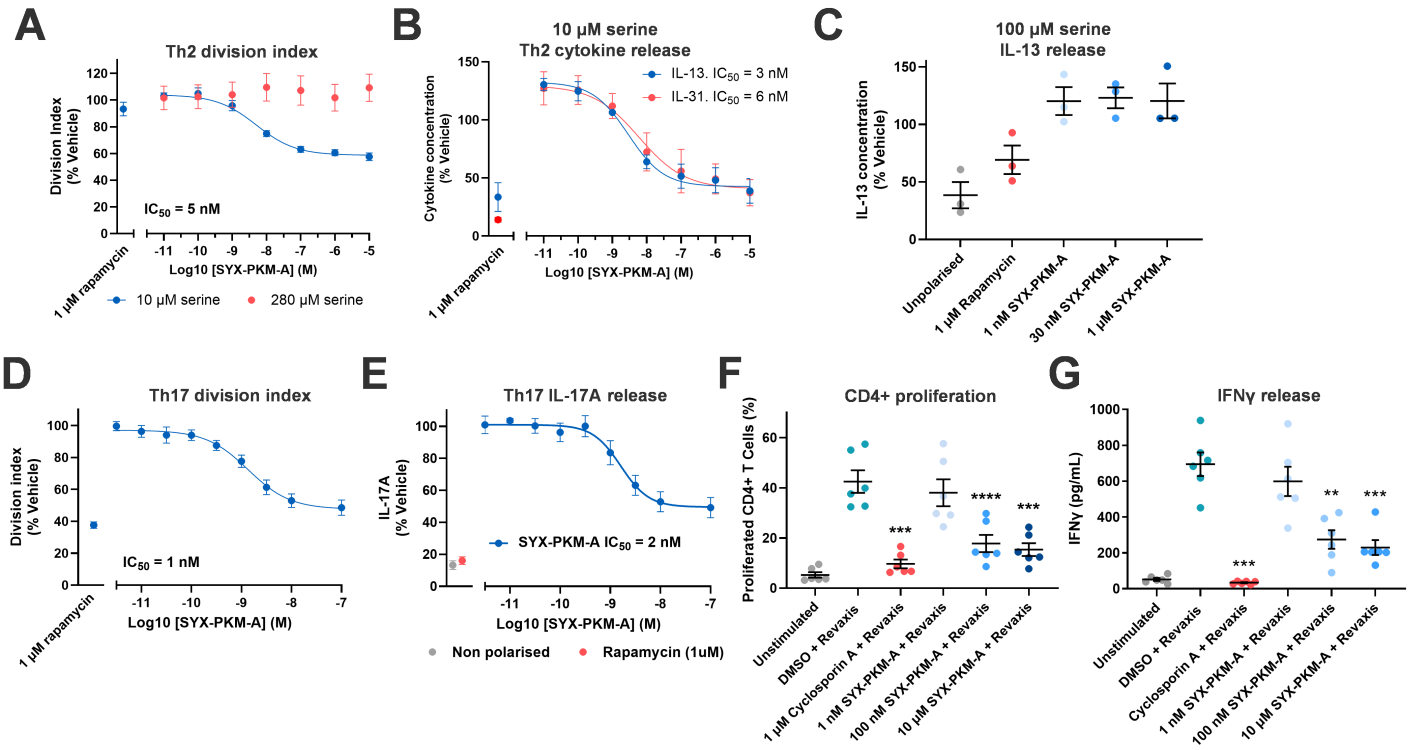


Figure 3

PKM2 activation inhibits the function of human Th2,Th17 and IFNγ-releasing cells

A. Stimulated Th2 division index after 5 days incubation with SYX-PKM-A in media containing either high or low serine. 1 µM rapamycin was used as a positive control for cytokine release. Data is presented with normalisation to the DMSO control (100%) showing mean ± SEM of 6 donors. B. IL-13 and IL-31 release from the experiment described in 3A in media with 10 µM serine. C. IL-13 release from Th2 cells after 5 days incubation with SYX-PKM-A in media with 100 µM serine. D. Stimulated human Th17 division index after 6 days incubation with SYX-PKM-A in media containing 10 µM serine. 1 µM rapamycin was used as a positive control. Data is presented with normalisation to the DMSO control (100%) showing mean ± SEM of 7 donors. E. IL-17A release from the experiment described in 3D. F. Percentage proliferation of CD4+ T cells in a PBMC culture stimulated with Td-IPV and IL-2 for 13 days in media containing 10 µM serine. 1 µM cyclosporin A was used as a positive control. Data is presented as mean ± SEM of 6 donors. G. IFNγ release from the experiment described in 3F. One way ANOVA with Dunnett's post-test * $p < 0.05$, ** $p < 0.01$, *** $p < 0.001$, **** $p < 0.0001$.

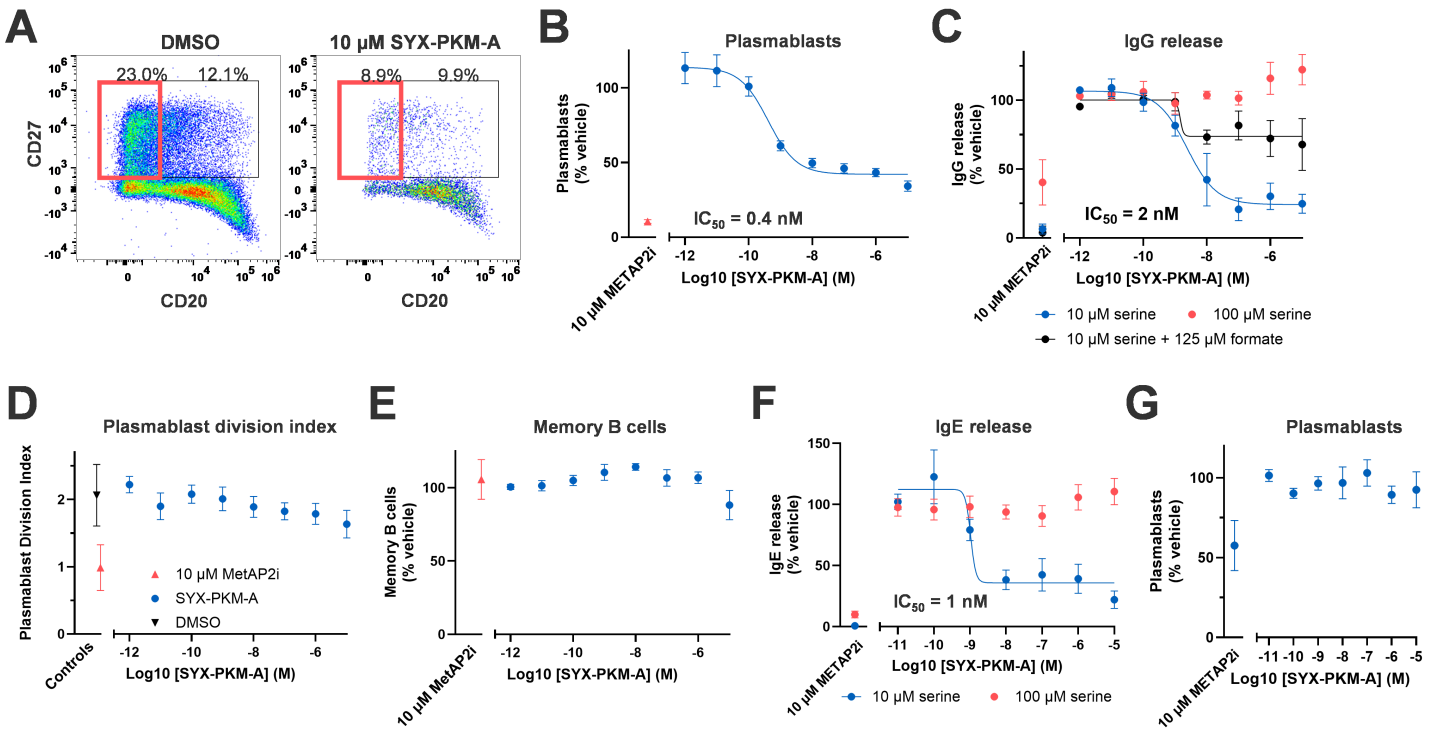


Figure 4

PKM2 activation inhibits human B cell function

A and B. Plasmablasts following stimulation of human B cells to promote IgG release and treated with SYX-PKM-A for 7 days in media containing 10 µM serine. A METAP2 inhibitor was used as an assay positive control at 10 µM. Data is presented as mean ± SEM of 4 donors. C. IgG release from the experiment described in 4A. The assay was also performed in media containing 100 µM serine or 10 µM serine with 125 µM formate. D. Plasmablast division index and E. Memory B cells from the experiment described in 4A. F. IgE release following stimulation of B cells to promote IgE release for 7 days with

SYX-PKM-A treatment in media containing 10 μM serine or 100 μM serine. G. Plasmablasts from the experiment described in 4F. Data is presented as mean ± SEM of 8 donors.

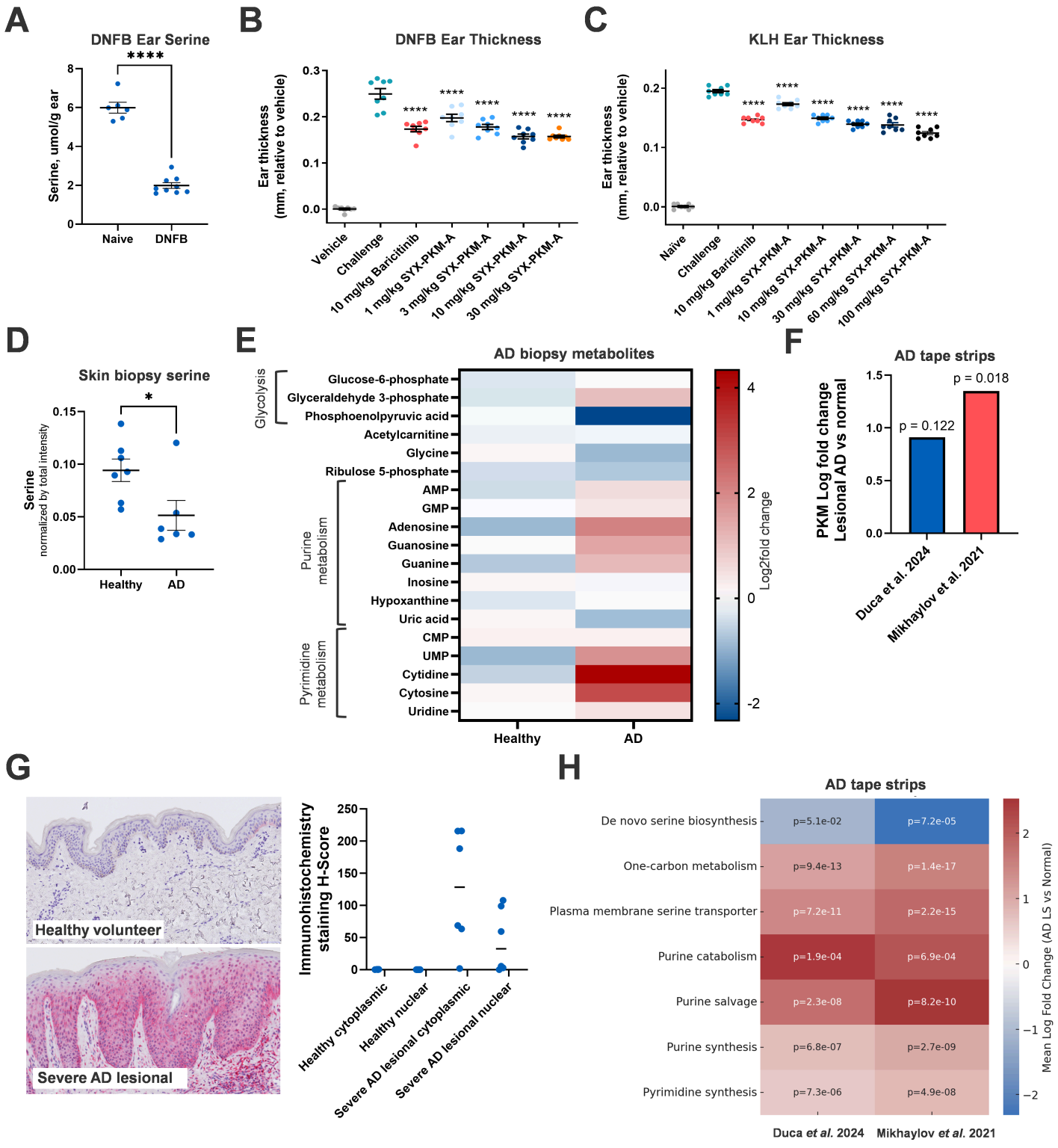


Figure 5

High serine demand in atopic dermatitis and mouse model of inflammation

A. Ear serine measured 24 hours after DNFB challenge. BALB/c mice were sensitised with DNFB on the back on days 0 and 1, followed by challenge on the ear on day 5. Data is presented as mean ± SEM of at least 6 animals. B. Ear thickness measured 24 hours after DNFB challenge. Mice were treated with a single dose of 10 mg/kg baricitinib PO, or SYX-PKM-A at 1 mg/kg, 3 mg/kg, 10 mg/kg or 30 mg/kg PO at 1 hour prior to the challenge. C. Ear thickness measured 24 hours after KLH challenge. Mice were treated with a single dose of 10 mg/kg baricitinib PO, or SYX-PKM-A at 1 mg/kg, 10 mg/kg, 30 mg/kg , 60 mg/kg or 100 mg/kg PO at 1 hour prior to the challenge. One way ANOVA with Dunnett's post-test with comparison of treatment groups to the challenge group * $p < 0.05$, **** $p < 0.0001$. D. Serine measured in healthy and AD skin biopsies. Data is presented as mean ± SEM of 7 human donors per group. E. Metabolites in healthy and AD skin biopsies with 7 human donors per group. F. PKM expression in the Duca *et al.* 2024 and Mikhaylov *et al.* 2021 AD skin tape strip RNAseq datasets. G. AD and healthy PKM2 immunohistochemistry with H-score staining quantification presented for 6 donors per group. H. Gene expression in the Duca *et al.* 2024 and Mikhaylov *et al.* 2021 AD skin tape strip RNAseq datasets.

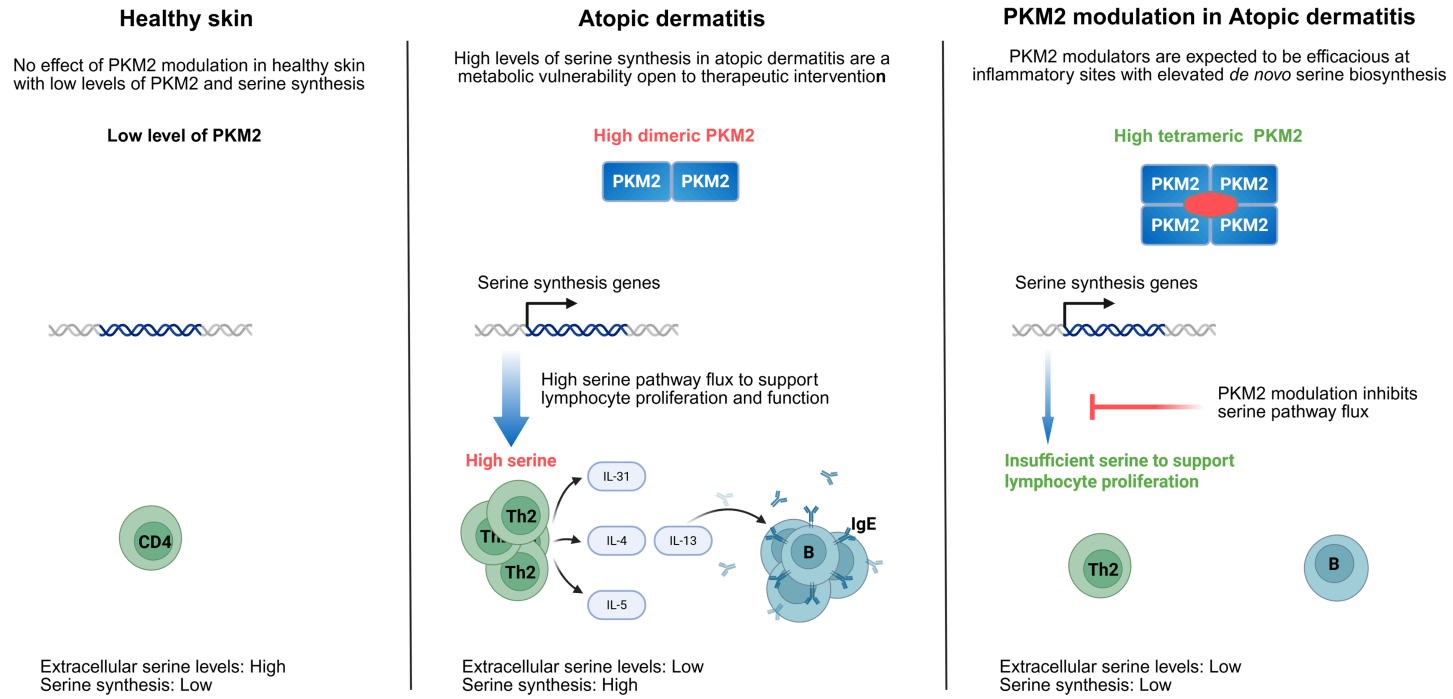


Figure 6

Serine determines tissue targeted efficacy of PKM2 modulators in atopic dermatitis

PKM2 modulation with SYX-PKM-A is not predicted to impact healthy skin, which has low levels of PKM2 and low serine demand. AD has high serine demand, as evidenced by reduced serine levels and high expression of serine transporter, one carbon metabolism and nucleotide metabolism genes in AD skin. PKM2 modulation drives inflammatory dimeric PKM2 to anti-inflammatory tetrameric PKM2. This is predicted to be efficacious in AD skin by inhibition of serine pathway flux in lymphocytes, reducing

proliferation and release of inflammatory cytokines and IgE. Figure prepared using https://BioRender.com

Supplementary Files

This is a list of supplementary files associated with this preprint. Click to download.

- SupplementaryExperimentalProcedures.docx
- SupplementaryFigures.docx